

Structure of light neutron-rich nuclei through Coulomb dissociation

U DATTA PRAMANIK, T AUMANN, D CORTINA, H EMLING, H GEISSEL, M HELLSTRÖM, R HOLZMANN, N IWASA, Y LEIFELS, G MÜNZENBERG, M REJMUND, C SCHEIDENBERGER, K SÜMMERER, A LEISTENSCHNEIDER¹, Th W ELZE¹, A GRÜNSCHLOSS¹, S ILIEVSKI¹, K BORETZKY², J V KRATZ², R KULESSA³, E LUBKIEWICZ³, E WAJDA³, W WALUS³, P REITER⁴ and H SIMON⁵

Gesellschaft für Schwerionenforschung, Planckstr. 1, D-64291 Darmstadt, Germany

¹Institut für Kernphysik, J. W. Goethe-Universität, D-60486 Frankfurt, Germany

²Institut für Kernchemie, Johannes Gutenberg-Universität, D-55099 Mainz, Germany

³Instytut Fizyki, Uniwersytet Jagielloński, PL-30-059 Kraków, Poland

⁴Sektion Physik, Ludwig-Maximilians-Universität, D-85748 Garching, Germany

⁵Institut für Kernphysik, Technische Universität, D-64289 Darmstadt, Germany

Abstract. Coulomb breakup of neutron-rich nuclei around mass $A \sim 20$ has been studied experimentally using secondary beams (~ 500 – 600 MeV/u) of unstable nuclei produced at GSI. The spectroscopic factor deduced for the neutron occupying $s_{1/2}$ level in ^{15}C ground state is consistent with the earlier reported value. The data analysis for Coulomb breakup of ^{17}C shows that most of the cross section yields the ^{16}C core in its excited state. For $^{17-22}\text{O}$, the low-lying E1 strength amounts up to about 12% of the energy weighted dipole sum rule strength depending on neutron excess. The cluster sum rule limit with ^{16}O as a core is almost exhausted for $^{17,18}\text{O}$, while for more neutron rich isotopes the strength with respect to that limit decreases.

Keywords. Coulomb breakup; exotic nuclei.

PACS Nos 21.10.Pc; 23.20.-g; 25.60-t

1. Introduction

The physics of exotic nuclei has attracted much interest during the past decade. The properties of nuclei with large neutron excess have turned out to be very different compared to those of stable nuclei in many respects. One outstanding observation in exotic nuclei is the halo structure. The halo structure arises from the low binding energy of valence nucleons, which can tunnel through the potential barrier and have an appreciable probability to be localized at a distance much larger than the mean radii of nuclei. First experimental evidence of this feature was deduced from large matter radii, inferred from interaction cross section measurements [1]. Another experimental signature was obtained from narrow momentum distributions of the fragments after one-neutron removal reactions. Such narrow momentum distributions are inherent to the large spatial distribution of the loosely bound

halo neutrons [2,3]. Moreover, the loosely bound valence nucleons are strongly coupled to the particle continuum, yielding the phenomenon of low-lying multipole strength, not observed in stable nuclei. Experimentally, low-lying dipole strength was observed for the halo nuclei ${}^6\text{He}$ [4], ${}^{11}\text{Li}$ [5–7], ${}^{11}\text{Be}$ [8] and ${}^{19}\text{C}$ [9]. To explain this enhancement of low-lying dipole strength in neutron-rich nuclei, two types of mechanisms have been discussed. One is the excitation of the soft dipole resonance which may occur due to the oscillation of the core against loosely bound nucleons. The other is the direct breakup mechanism leading to continuum final states. In this paper, we shall present our recent experimental results on both, single particle and collective properties of light neutron-rich nuclei. As an experimental probe we used the electromagnetic excitation of secondary beams of exotic nuclei at high energy passing by a high- Z target. This type of excitation favours E1 transitions with only small contributions from E2 transitions. Experimental results on the dipole response of the neutron rich carbon isotopes ${}^{15,17}\text{C}$ and the oxygen isotope chain with $A = 17$ to 22 are presented.

2. Experimental method

The radioactive beams were produced in a fragmentation reaction of a primary ${}^{40}\text{Ar}$ beam, delivered by the synchrotron SIS at GSI, Darmstadt, impinging on a beryllium (4.0 g/cm^2) target. The fragments were separated using the fragment separator FRS [10]. In two settings, a degrader was inserted in the midplane of the FRS. In these cases only ${}^{17,18}\text{O}$ and ${}^{19,20}\text{O}$, respectively, were transported to the experimental area. Figure 1 shows a schematic view of our experimental setup. In a third setting without degrader and optimized for ${}^{22}\text{O}$, the beam contained various isotopes with similar mass-to-charge ratio (A/Z) ranging from Be up to F. The secondary beams were identified uniquely by means of energy-loss and time-of-flight measurements. Figure 2 shows composition of incident ‘cocktail’ beam. The trajectory of the particle was measured by position sensitive Si pin-diodes placed before and after the secondary target. Behind the target, the fragments were deflected by a large gap dipole magnet (ALADIN). By using energy-loss and time-of-flight measurements, as well as position measurements before and after the dipole magnet, the nuclear charge, velocity, scattering angles and the mass of the fragments were determined. The position of the fragments after ALADIN was measured by fiber detectors [11]. The neutrons stemming from the excited projectile or excited projectile-like fragments were kinematically focussed into the forward direction and were detected with high efficiency in the LAND neutron detector [12]. This detector was placed at zero degree about 11 m downstream from the target and covers a horizontal and vertical angular range of about ± 80 mrad. In order to detect γ -rays, the target was surrounded by the 4π Crystal Ball spectrometer, consisting of 160 NaI detectors.

3. Data analysis and results

By measuring the four-momenta of all decay products of the projectile after inelastic scattering followed by breakup, the excitation energy of the nucleus is determined. The Coulomb dissociation cross section with the Pb (1.8 g/cm^2) target was obtained after

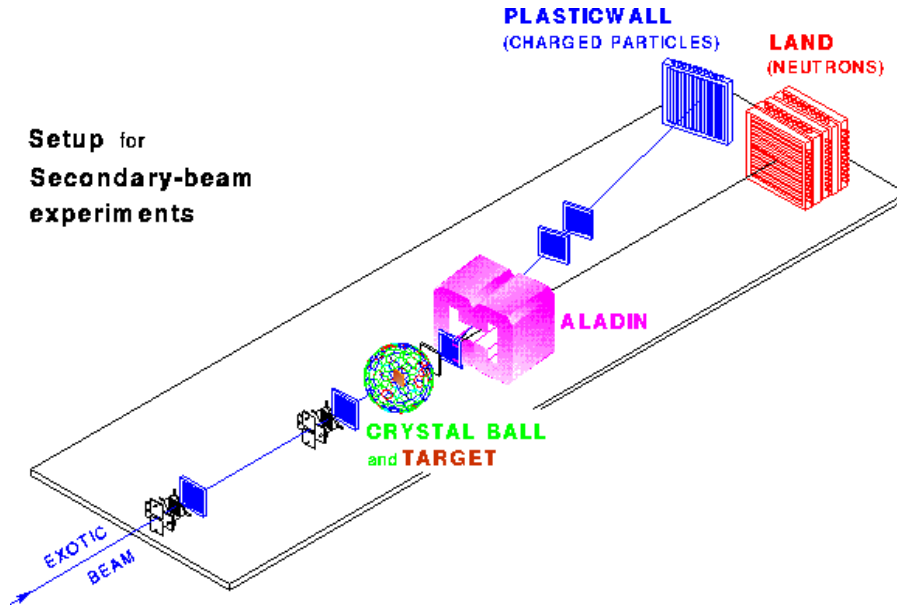


Figure 1. Schematic view of the setup in the experimental area.

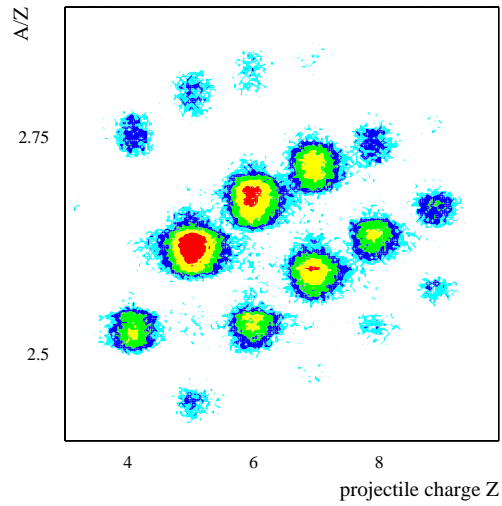


Figure 2. Composition of the secondary 'cocktail' beam.

subtracting nuclear contributions determined from the data with a C (0.573 g/cm²) target applying a proper scaling of the cross sections (for details see [13]). From the measured differential cross sections $d\sigma/dE^*$ (excitation energy E^*) for electromagnetic excitation, the $B(E1)$ -strength distributions were deduced on the basis of the semiclassical approximation [14,15].

4. Direct breakup of ^{15,17}C

According to the direct breakup model, the nucleus is considered as a core plus a loosely bound nucleon. The neutron separation energies of ^{15,17}C amount to 1.218 and 0.729 MeV, respectively, and are thus much smaller than the binding energies of core neutrons. When a projectile moves with very high velocity passing by a high- Z target, it is excited by absorbing virtual photons due to the time-dependent Coulomb field. The differential cross section may be written as (see [9,16]):

$$\frac{d\sigma}{dE^*} = \left(\frac{16\pi^3}{9\hbar c} \right) N_{E1}(E^*) \sum_m |\langle q | (Ze/A)rY_m^1 | \psi(r) \rangle|^2. \quad (1)$$

$N_{E1}(E^*)$ represents the number of equivalent dipole photons of the target Coulomb field, computed in a semiclassical approximation [14,15]. $\psi(r)$ represents the ground state wave function of the projectile. $\langle q |$ describes the final state where the neutron is in the continuum and it is approximated by a plane wave. The single particle wave functions forming the ground state have been derived from a Woods–Saxon potential with parameters $r_0 = 1.25$ fm and $a = 0.7$.

It is clear from the above relation that the dipole strength distribution is very sensitive to the single particle wavefunction which in turn depends on the orbital angular momentum and the binding energy of the valence neutron. Thus, comparing the experimental Coulomb dissociation cross section with the calculated one, information on the ground state properties such as orbital angular momentum of the valence nucleon and the corresponding spectroscopic factor may be gained. The core state to which the neutron is coupled can be identified by the characteristic γ decay.

The ground state spin of the ¹⁵C I^π is known to be $I^\pi = 1/2^+$ and a spectroscopic factor for the neutron in the s orbital of 0.88 was obtained from the ¹⁴C(d, p)¹⁵C reaction [17]. A narrow momentum distribution (67 ± 3 MeV/c) of the fragment ¹⁴C was observed after one neutron knockout reactions [3]. The matter radius, as inferred from the measured interaction cross sections, however, seems only marginally larger than that of the core nucleus [18]. These somewhat conflicting results encouraged us to investigate ¹⁵C.

Our data analysis [19,20] shows that the overwhelming part of the breakup cross section leaves the ¹⁴C core in its ground state and only a small fraction of ¹⁴C fragments appear in excited states, as could be deduced from the corresponding γ -ray spectra. The differential cross section $d\sigma/dE^*$, analysed as described above, is consistent with a predominant ¹⁴C(0^+) \otimes $\nu_{S_{1/2}}$ configuration and also, within minor deviations, with the spectroscopic factor extracted from the (d, p) reaction. Figure 3 shows the sum energy spectra of the γ decay from ¹⁴C fragments. The lower part of figure 3 shows $d\sigma/dE^*$ for electromagnetic excitation of ¹⁵C followed by decay into a neutron and a ¹⁴C fragment in its ground state. Contributions from excited states are subtracted. The experimentally observed shape of the

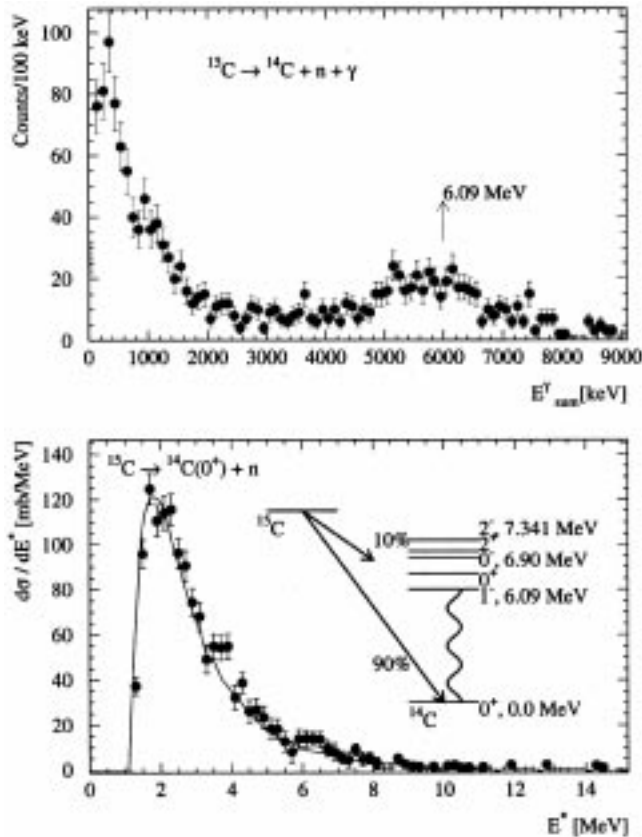


Figure 3. Top: γ -sum energy spectrum as measured in coincidence with ^{14}C fragments after breakup of ^{15}C . Bottom: Coulomb dissociation cross section as a function of excitation energy (E^*) of ^{15}C (605 MeV/u) breaking up into a neutron and a ^{14}C fragment in its ground state. Contributions involving excited states as well as contributions from nuclear excitations are subtracted. The solid curve reflects the results from calculation on the basis of direct breakup model (see text). The data are not corrected for efficiency and acceptance of the neutron detector system, but the instrumental response function was folded into the calculation.

spectrum is in perfect agreement with the calculation (solid curve) where a s -wave neutron single particle wavefunction coupled to the ^{14}C ground state was adopted. From the absolute cross section, a spectroscopic factor 0.72 is deduced. In the lower panel of figure 3 we also show the relative Coulomb breakup cross sections for the population of different core states. We would like to mention that we have applied the same method to ^{14}B [21], which was part of the mixed secondary beam, and obtain a spectroscopic factor consistent with that from independent measurements [22].

The ground state spin of ^{17}C is not fully established experimentally. Since the last valence neutron can occupy $1s_{1/2}$, $0d_{3/2}$ or $0d_{5/2}$ orbitals, the ground state spin could be $1/2$, $3/2$ or $5/2$. Shell model calculations predict three low-lying (triplet) levels with

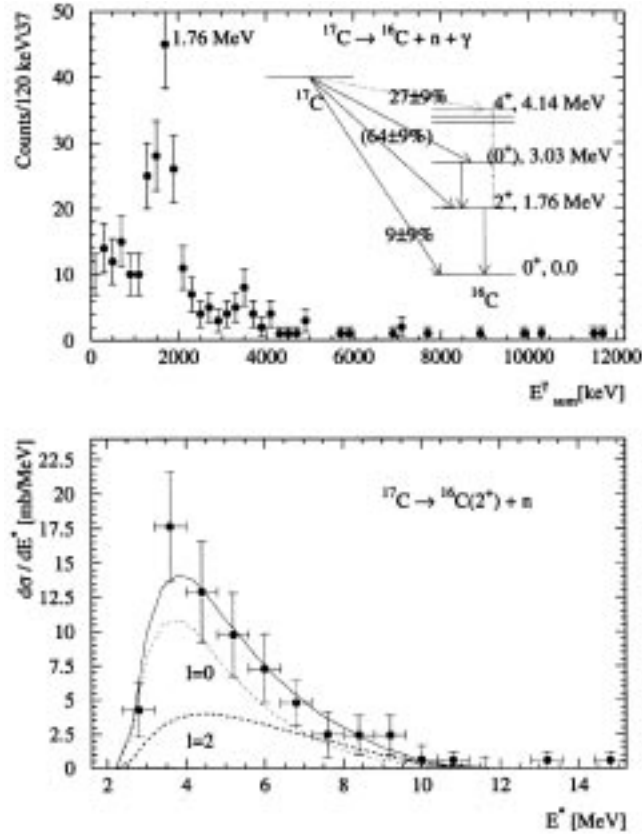


Figure 4. Top: Sum energy of γ decay transitions from ^{16}C after breakup of ^{17}C . Bottom: Coulomb dissociation cross section as a function of excitation energy (E^*) of ^{17}C in coincidence with the 1.766 MeV γ transition ($^{16}\text{C}(2^+ \rightarrow 0^+)$). For comparison with calculated cross sections (solid and dashed lines), see the text.

these spins. Warburton and Millener [23] showed that the analysis of the γ -ray spectra following β -decay of this isotope seems to exclude $5/2^+$ as ground state. A comparison of the measured β -decay half-life of this isotope [24] with the theoretical prediction for a Gamow–Teller β -decay, however, allows both $3/2$ or $5/2$ as ground state spin. It may be interesting to notice that though the neutron separation energy is smaller than in the case of ^{15}C , relatively a broad momentum distribution (141 ± 6 MeV/c) of the fragment (^{16}C) was observed in one neutron knockout reactions [2,3].

Our experimental data for Coulomb breakup of ^{17}C show that most of the cross section yields the ^{16}C core in its excited state with $I^\pi = 2^+$, or excited states at excitation energies of around 3–4 MeV. Only a very small part of the cross section leaves the core in its ground state. Figure 4 shows the sum energy spectra of the γ decay from ^{16}C fragments. In the upper panel of the figure we also show the relative Coulomb breakup cross sections for the population of different core states. The lower part of figure 4 shows $d\sigma/dE^*$

for electromagnetic excitation of ^{17}C in coincidence with the 1.766 MeV γ transition ($^{16}\text{C}(2^+ \rightarrow 0^+)$) without acceptance and efficiency corrections for the neutron detector. These corrections, however, are taken into account in the calculated cross sections using detailed detector response simulations. A proper choice of relative contributions from wave functions involving $l = 0$ and $l = 2$ neutrons, as shown in the figure, can reproduce the data well. Thus, $^{16}\text{C}(2^+) \otimes \nu_{s,d}$ can be considered as the dominant ground state configuration of ^{17}C [19] and a $1/2^+$ ground state spin of ^{17}C can be ruled out. In consequence, $3/2^+$ and $5/2^+$ are the possible ground state spins of ^{17}C . The Coulomb dissociation cross section which populates ^{16}C in its ground state is ($\sim 9 \pm 9$ mb) very small. The shell model calculations [25] quote the spectroscopic factor of 0.7 and 0.03 for neutron considering $^{16}\text{C}(0^+) \otimes \nu_{d_{5/2}}$ and $^{16}\text{C}(0^+) \otimes \nu_{d_{3/2}}$ as ground state configurations, respectively. The direct break up model delivers a cross section of 107 mb for a $^{16}\text{C}(0^+) \otimes \nu_d$ configuration with spectroscopic factor of unity. Thus, our experimental result favours $I^\pi = 3/2^+$ as ground state spin of ^{17}C . It should be noticed that our results are in agreement with those observed from an independent method, i.e knockout reactions [25].

5. E1 strength distribution of neutron-rich oxygen isotopes

The electromagnetic excitation to the continuum with subsequent neutron decay was investigated systematically for neutron-rich oxygen isotopes up to ^{22}O [26]. Using unstable beams of energies of 500 to 600 MeV/u, the dipole strength can be studied up to about 30 MeV in excitation energy. ^{16}O is a strongly bound doubly magic nucleus. For the heavier isotopes one may expect a decoupling of valence neutrons from the inert ^{16}O core. The separation energy for the last neutron in the even isotopes $A = 20$ to 24 is 7 to 8 MeV and less (3 to 4 MeV) for odd-even isotopes, compared to 16 MeV for ^{16}O . Thus, the neutron-rich oxygen isotopes might be considered as candidates to show soft-dipole excitation at excitation energies well below that of giant dipole resonance which is observed at energies of 20–30 MeV in ^{16}O .

For ^{18}O , we have compared our measured differential Coulomb excitation cross section with that, derived from photo absorption measurements [27–29]. The comparison shows good agreement with our data.

In figure 5, the evolution of the integrated low-lying strength for oxygen isotopes is summarized. The experimental data are normalized to the values of the classical dipole sum rule S_{TRK} and to that of the dipole cluster sum rule S_{clus} . The latter [30] can be written as

$$S_{\text{clus}} = S_{\text{TRK}} \times \frac{Z_c N_v}{A_c N}, \quad (2)$$

where S_{TRK} stands for the classical energy weighted Thomas–Reiche–Kuhn dipole sum rule [31] limit, and the indices c and v refer to the core and valence nucleons, respectively. It may be noted that the requirement for application of the cluster sum rule is to identify the dipole strength associated with the relative motion between core and valence nucleons. In figure 5, the energy-weighted dipole strength integrated up to 15 MeV excitation energy as fractions of the classical and cluster dipole sum rules are shown. For this integration limit, the low-lying dipole strength for oxygen isotopes exhausts up to 12% of the classical sum

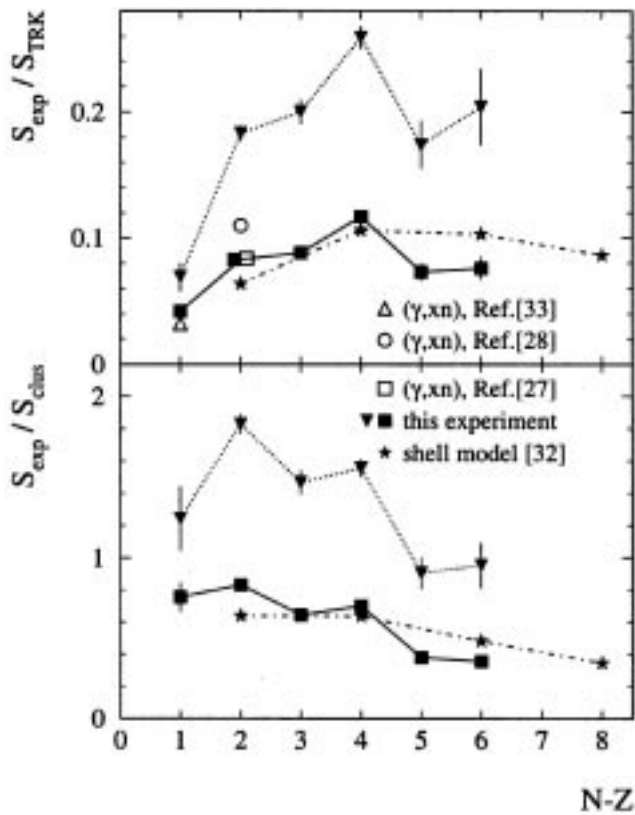


Figure 5. Evolution of integrated dipole strength S_{exp} in units of the TRK sum rule S_{TRK} (upper panel) and of the cluster sum rule S_{clus} (lower panel) for oxygen isotopes as a function of the neutron excess $N-Z$. The filled squares and triangles denote the dipole strength integrated up to 15 and 20 MeV, respectively. The data are compared to a shell model calculation by Sagawa and Suzuki (integrated up to 15 MeV excitation energy). For the stable $^{17,18}\text{O}$ isotopes results from photo absorption measurements are shown for comparison (open symbols).

rule. The lower part of the figure shows that the cluster sum rule limit (with ^{16}O taken as the core) is exhausted $\sim 80\%$ for $^{17,18}\text{O}$. But for the more neutron-rich nuclei, dipole strength as a fraction of S_{clus} decreases continuously. On the other hand, one observes that if the strength is integrated up to 20 MeV, it exceeds the cluster sum rule limit. Thus, core excitations plays already a role in this energy region, while for ^{16}O the integrated photo-neutron cross section between 15 to 20 MeV corresponds to 1.6% [34] of S_{TRK} only. It thus appears that a strict separation into a core and valence nucleon sector is not applicable.

6. Summary

We have shown that Coulomb dissociation is a powerful tool to explore the single particle structure as well as collective properties of exotic nuclei. Differential Coulomb dissocia-

tion cross sections for neutron rich nuclei in the mass region around $A \sim 20$ were deduced. For $^{15,17}\text{C}$, the observed low-lying dipole strength can be explained by direct transitions into the continuum. For ^{15}C the main ground state configuration is $^{14}\text{C}(0^+) \otimes \nu_s$. The deduced spectroscopic factor is consistent with that obtained from (d, p) reactions. For ^{17}C , it is found that the dominant ground state configuration involves a mixture of s and d wave neutrons coupled to the (2^+) first excited state of the ^{16}C core. A systematic investigation of the dipole strength distribution for $^{17-22}\text{O}$ isotopes was performed. A clear separation of dipole strength associated to core excitations and to the relative motion between core and valence nucleons is not observed.

Acknowledgements

This work was supported by the German Federal Minister for Education and Research (BMBF) under Contracts 06 OF 838 and 06 MZ 864, and by GSI via Hochschulzusammenarbeitsvereinbarungen under Contracts OFELZK, MZKRAK, and partly supported by the Polish Committee of Scientific Research under Contract No. 2PB03 144 18.

References

- [1] I Tanihata, *Phys. Rev. Lett.* **55**, 2676 (1985)
- [2] T Bauman *et al*, *Phys. Lett.* **B439**, 256 (1998)
- [3] D Bazin *et al*, *Phys. Rev.* **C57**, 2156 (1998)
- [4] T Aumann *et al*, *Phys. Rev.* **C59**, 1252 (1999)
- [5] D Sackett *et al*, *Phys. Rev.* **C48**, 118 (1993)
- [6] F Shimoura, T Nakamura, M Ishihara, N Inabe, T Kobayashi, T Kubo, R H Siemssen, I Tanihata and T Watanabe, *Phys. Lett.* **B348**, 29 (1995)
- [7] M Zinser *et al*, *Nucl. Phys.* **A619**, 151 (1997)
- [8] T Nakamura *et al*, *Phys. Lett.* **B331**, 296 (1994)
- [9] T Nakamura *et al*, *Phys. Rev. Lett.* **83**, 1112 (1999)
- [10] H Geissel *et al*, *Nucl. Instrum. Methods* **B70**, 286 (1992)
- [11] J Cub, *et al*, *Nucl. Instrum. Methods* **A402**, 67 (1998)
- [12] T Blaich *et al*, *Nucl. Instrum. Methods* **A314**, 136 (1992)
- [13] T Aumann *et al*, *Nucl. Phys.* **A649**, 297c (1999)
- [14] A Winther and K Alder, *Nucl. Phys.* **A319**, 518 (1979)
- [15] C A Bertulani and G Baur, *Phys. Rep.* **163**, 299 (1988)
- [16] D Ridikas, M H Smedberg, J S Vaagen and M V Zhukov, *Nucl. Phys.* **A628**, 363 (1998)
- [17] J D Goss, A A Rollefson, C P Browne, R A Blue and H R Weller, *Phys. Rev.* **C8**, 514 (1973)
- [18] A Ozawa *et al*, RIKEN Preprint RIKEN-AF-NP-376, November 2000
- [19] U Datta Pramanik *et al*, GSI, Preprint 2000-18 (2000); to be published in *Nucl. Phys.*
- [20] U Datta Pramanik *et al*, manuscript under preparation
- [21] U Datta Pramanik *et al*, *Proc. of Int. Symp. on Nuclear Structure Phys.*, Göttingen, Germany, March, 2001; to be published by World Scientific Publishing Company
- [22] V Guimaraes *et al*, *Phys. Rev.* **C61**, 064609 (2000)
- [23] E K Warbourton and D J Millener, *Phys. Rev.* **C39**, 1120 (1992)
- [24] M S Curtin, L H Harwood, J A Nolen, B Sherrill, Z Q Xie and B A Brown, *Phys. Rev. Lett.* **56**, 34 (1986)
- [25] V Maddalena *et al*, *Phys. Rev.* **C63**, 024613 (2001)

- [26] A Leistenschneider *et al*, *Phys. Rev. Lett.* (submitted to)
- [27] U Kneissl, K H Leister, H O Neidel and A Weller, *Nucl. Phys.* **A272**, 125 (1976)
- [28] J G Woodworth, K G McNeill, J W Jury, R A Alvarez, B L Berman, D D Faul and P Meyer, *Phys. Rev.* **C19**, 1667 (1979)
- [29] H Harada, Y Shigetome, H Ohgaki, T Noguchi and T Yamazaki, *Phys. Rev. Lett.* **80**, 33 (1998)
- [30] H Sagawa and M Honma, *Phys. Rev. Lett.* **251**, 17 (1990)
Yoram Alhassid, Moshe Gai George and F Bertsch, *Phys. Rev. Lett.* **49**, 1482 (1982)
- [31] A Bohr and B R Mottelson, *Nuclear Structure* (1975) vol. 2
- [32] H Sagawa and T Suzuki, *Phys. Rev.* **C59**, 3116 (1999)
- [33] J W Jury, B L Berman, D D Faul, P Meyer and J G Woodworth, *Phys. Rev.* **C21**, 503 (1980)
- [34] E G Fuller, *Phys. Rep.* **127**, 187 (1985)
A Vessi re, H Beil, R Bergere, P Carlos, A Leprerre and A de Miniac, *Nucl. Phys.* **A227**, 513 (1974)